LIP-STUDENTS-22-18

High-precision timing detectors for the HL-LHC

Beatriz Amorim[1,a]

[1] *Faculdade de Ciências, Lisboa, Portugal*

Project supervisors: Tahereh Niknejad and Cristóvão da Cruz e Silva

November 1, 2022

Abstract. During the High Luminosity LHC (HL-LHC) era there will be much higher collision rates that will far exceed the capabilities of the existing CMS detector, which will consequently require significant upgrades to continue to function efficiently. The MIP Timing Detector (MTD) will be added to CMS to help meet the challenge of high luminosity, by giving us another dimension to use - time. A resolution of 30 (60) ps for MIP signals at the beginning (end) of HL-LHC operation is expected. Dedicated ASIC electronics (TOFHIR2) is used in the readout of SiPM arrays coupled to LYSO crystal bars. In this work the TOFHIR2B version of the chip associated to SiPMs has been characterized experimentally at the begining and the end of HL-LHC life.

KEYWORDS: MTD,TOFHIR2B,Time

1 Introduction

In order to maximise the probability of the protons colliding with one another, the LHC tries to pack as many protons as it can into the beam and squeeze it as narrowly as possible. The narrower the beam and the more protons in it, the higher the "luminosity" will be. For LHC, the nominal luminosity is of $L = 1 \times 1034 cm^2 s^{-1}$, while for the High Luminosity LHC (HL-LHC), the nominal luminosity would be $L = 5 \times 10^{34} cm^2 s^{-1}$. And so, the goal is to reach an ultimate scenario of luminosity : $L = 7.5 \times 10^{34} cm^2 s^{-1}$ [1]. This will provide 30 % more integrated luminosity, at the cost of producing 200 collisions per beam crossing. Hard interactions of interest to CMS, those that probe energy scales ranging from a few GeV to several TeV, occur in far fewer than 1% of the total beam crossings but will always be accompanied by an average of 140–200 additional interactions. The spatial overlap of tracks and energy deposits from the additional collisions can degrade the identification and the reconstruction of the hard interaction and can increase the rate of false triggers. In addition, the higher collision rate integrated over time results in more radiation damage than can be tolerated by some of the existing subdetectors.The upgraded detector must survive and function efficiently in this much harsher radiation and high pileup environment and must transport a much higher rate of data off the detector to be recorded for analysis [1]. The MIP Timing Detector (MTD) will give timing information for MIPs with 30–40 ps resolution at the beginning of HL-LHC operation in 2026, degrading slowly as a result of radiation damage to 50–60 ps by the end of HL-LHC operations[1]. This time information will be assigned to disentangle overlapping vertices[2], which are proton interactions.

1.1 MIP timing detector

The MIP timing detector will consist of a central Barrel Timing Layer (BTL), which is a thin standalone detector based on LYSO:Ce crystals read-out with Silicon Photomultipliers (SiPMs). Dedicated ASIC electronics is used in the readout. The readout solution uses the new TOFHIR2 chip. The endcap region of the MTD, called the Endcap Timing Layer (ETL),is instrumented with radiation-tolerant Low Gain Avalanche Detectors (LGADs), but we were not studying them on this project.

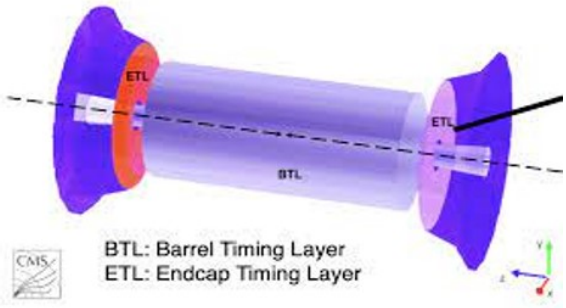

Figure 1. Schematic of the MTD

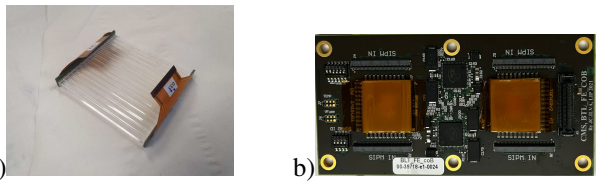

Figure 2. a) LYSO:Ce crystals bars; b) TOFHIR2B board.

Figure 3 shows a schematic on how the BTL works. The MIP particles interact with the crystal bars that produces light photons. The SiPM consists of a matrix of micro-cells all connected in parallel. Each micro-cell is a GM-APD and it represents the basic sensitive element of the SiPM. The amplitude of the current pulse produced by a micro-cell in response to one photon absorption (single-cell signal) is defined to one photonelectron. Depending on the laser there will be produced a lot photoelectrons, so one of the goals of this project is to get the time resolution

[a] e-mail: mariab.amorim@hotmail.com

for different number of photoelectrons. The number of photoelectrons is related to the current, by the following equation:

$$I = Npe \times f_{laser} \times G \times q_e \quad (1)$$

Where I is the the current measured with the laser, f is the frequency of the laser, q_e is the charge of the electron and G is the gain of the SiPM, which was set to 1.83×10^5 based on the over voltage that applied.

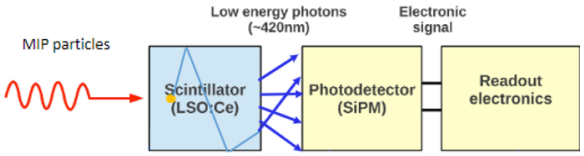

Figure 3. Schematic of BTL

1.2 TOFHIR2B

The BTL is read out by a dedicated ASIC, named TOFHIR (Time-of-flight, High Rate) chip, that delivers precision timing information for 32 SiPMs based on discrimination of the leading edges (LE) of their pulses followed by measurement with a time-to-digital converter (TDC). Each channel of the ASIC has three branches: two of them measure the time (T1 and T2) and the other measures the energy. For this project we will only be interested on the timing branch, more specifically T2. As you can see, in table 1, T1 and T2 both have different DAC LSB values which are set by range settings and the difference between the two timing branches is that T2 has a bigger range than T1.

Table 1. Diferent ranges for diferent thresholds settings for the two timing branches.

T1	I(μA)	T2	I(μA)
0	154	0	313
1	313	1	625
2	450	2	940
3	625	3	1250

In each channel of the ASICs we have an amplifier with DCR cancellation circuit followed by a current discriminator. The main goal of the DCR cancellation circuit is to mitigate the SiPM dark noise and the baseline fluctuations. To be more precise, due to the radiation damage, the SiPM produces dark current noise. To reduce the impact of DCR noise on the rising edge of the pulse we added this block. In this block, an inverted and delayed current pulse is added to the original pulse, so it makes the pulse shorter in width and smaller in amplitude. In this way we are cutting down the noise and it's impact on the rising edge of the pulse and, in particular, the beginning of the pulse, that is good for time measurements. Note that the dark current is due to thermally generated electron-hole pairs that initiate an avalanche inside the SiPM.

Then, we have the current discriminator. The discriminator measures the time that the signal goes above a certain threshold value. It does that by setting the threshold at different values and, then, we measured the crossing time of the signal at different threshold levels. We measured both of the crossing time of the rising edge and the falling edge of the signal, and then we reconstructed the full pulse shape including both of the edges. The delay line in the DCR cancellation module is made of a series of RC nets, where the delay that each RC nets applies is given by $R \times C$. We have one block with 7 RC nets in series and another one, under the other, with 7 RC nets in series. The two blocks have different values on the resistors,that allows to have a higher delay. Therefore,we have 14 delay settings (0 to 13). So, by increasing the delay the signal becomes bigger in amplitude and in with.
In addiction, the SiPM bias voltage is provided by the ALDO voltage regulator.

2 Development of the project

2.1 Calibration of TOFHIR2B

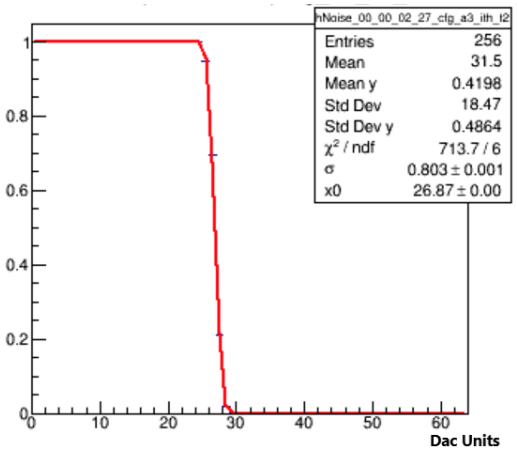

Figure 4. Plot made to study the noise and the baseline distributions more specifically the mean value for the baseline and sigma value for the noise.

The first step of this project was calibrating the board TOFHIR2B (figure 2b). The calibration is divided in three parts. The first one is the discriminator calibration. The goal of this calibration is to find out what are the baseline and the electrical noise values. This procedure is done by threshold scanning the noise and extracting the s-curve as seen in figure 4. The mean value of the fit of this plot is the baseline and the sigma represents the noise.
The second part of the calibration is the TDC and QDC calibration, but since we only used the timing branch we are only interested in the TDC calibration. The TDC calibration is done by externally generated signals that are routed to the digital front-ends. In this calibration the TDC is receiving a lot of pulses that arrive to the TDC at the same time, so, the dispersion that is present will be because of the TDC. We measure the resolution of the TDC for each channel of the ASIC.

The last part of the calibration is the pulse shape calibration. The goal of this calibration is to see the pulse shape on each channel to see if there is any problem in the analog part of the circuit. As mentioned earlier the time that the threshold DAC measures is the the time that the signal intersects the threshold values. So if we measure the time for all threshold values we get the pulse shape. Finally, we analyze the pulse shapes for all the channels.

2.2 Experimental Procedure

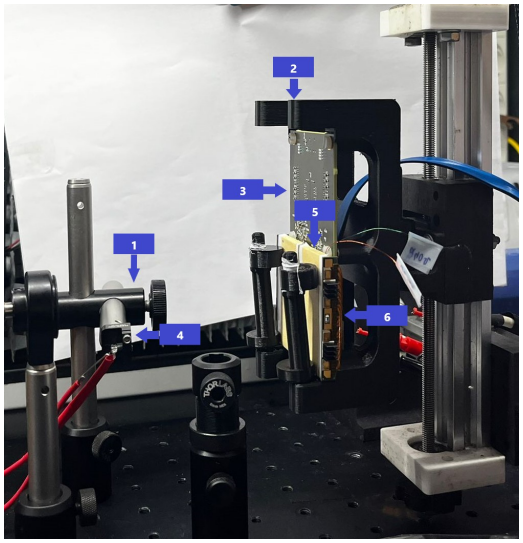

Figure 5. Setup used for this project.

Material

1. 375 nm UV Laser
2. Support made in a 3D Printer
3. TOFHIR2B
4. Blue LED
5. Module with the LYSO:Ce crystal bars
6. 2 SiPM arrays

After the calibration, we started collecting the data and for that we made an experimental set up, showned in figure 5. First we connected the LYSO crystals to the board. We use two SiPM arrays, with 16 pixels each, and each one was attached to one connector on one side. Then we put the board in a support that is connected to a motor controlled by arduino, so that we could be move it vertically. Using this moving support we aligned the crystal array with the laser such that the laser shines at the center of a particular bar. The whole setup is placed inside a light tight box. Using the temperature sensors on the SiPMs we kept the temperature stable at 19ºC. We used two multimeters to read the voltage on the 240Ω resistor of the AC coupling between one SiPM and the ASIC, and the Bias Voltage controlled by the ALDOs. From the voltage drop on 240Ω, we can measure the current ($V = 240 \times I$.) to calibrate the number of photoelectron.

Before starting to collect the data it is important to know what bias voltage do we want to see on the SiPM. In order to work on avalanche mode, we need to operate the SiPM above the breakdown voltage. For that we will use an over-voltage of 1.5 V which corresponds to the end of life condition. It's important to notice that the breakdown voltage of the SiPM varies with the temperature. We operated the SiPM at 39.83 V which is the breakdown voltage plus 1.5 V at 19ºC .

To do the time measurement we first took a look at the laser pulse shape by scanning the timing threshold at the output of the discriminator. This was important to see what range we should choose from table 1. In figures 6 and 7 one can see the difference between the pulse shapes using range 0 and 3. As can be seen, with range 0 we can not see the full form of the pulse, this is because the steps between the thresholds are smaller and so the threshold will not scan all the pulse. However, with a bigger range the full pulse shape is scanned (figure 7).

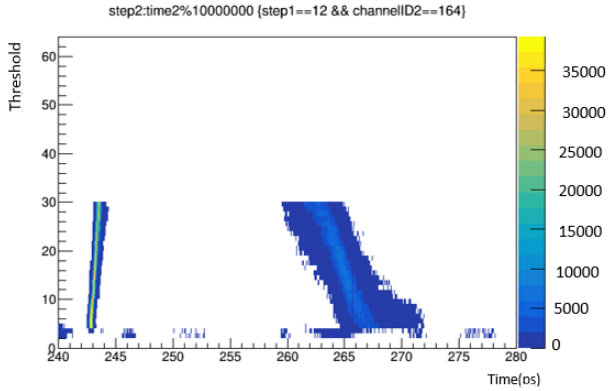

Figure 6. Pulse shape of a particular channel for a specific delay setting. The shape is extracted using T2 threshold scan and range 0.

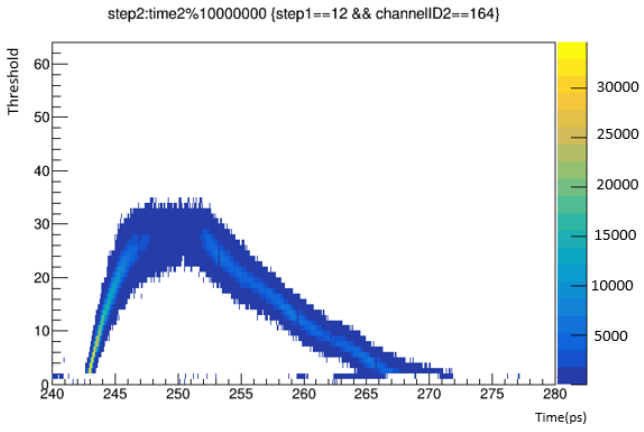

Figure 7. Pulse shape of a particular channel for a specific delay setting. The shape is extracted using T2 threshold scan and range 3.

Next we want to study the behavior of the time resolution when the MTD has already been exposed to a lot of radiation and dark current noise is present. Dark current noises are thermally generated electron-holes without the presence of any external light. The current in the presence of DCR is given by:

$$I = ((Npe \times f_{laser}) + f_{DCR}) \times G \times q_e \quad (2)$$

Where f_{DCR} is the frequency of the DCR. We used an LED light to emulate the DCR noise, because the LED ejects single photons randomly and we change the intensity of the LED such that it gives us the current corresponding to a particular frequency of the DCR.

We started by tuning the laser in order to have 6000 photoelectrons, and for that we tuned off the LED ($f_{DCR} = 0$). For LED calibration we turned off the laser. It's important to note that the current that passes trough the two 240Ω resistors, at the output of two SiPMs, of one bar, should be the same, so we started by checking this out. For that we connected the multimeters to both of the resistors, and with the laser off and the LED on, we made sure that the difference between the currents is within 5%. After this, we connected again one of the multimeters to the bias voltage and the other one was kept on the resistor. While the laser was off, we changed the LED intensity to see in the multimetre, that is connected to the 240 Ω, the voltage that is equal to $240 \times I$, where I is given by equation 2 with $f_{laser} = 0Hz$. Finally, after doing this, we turned on the laser and collect the data. We have done this project for the following DCR frequencies: 5 GHz, 10 GHz, 15 GHz, 20 GHz, 25 GHz, and 30 GHz. It is important to mention that by increasing the laser intensity the temperature on the SiPMs increases. Therefore, we either have to wait until the temperature becomes 19°C again; or see in what temperature it become stables and check the value of the breakdown voltage of the SiPM that match this temperature.

2.3 Time Resolution

The arrival time of the event is the time that the signal at the output of the ASIC crosses the threshold and, so, the higher the threshold the higher the crossing time. The time resolution of the bar is given by:

$$\sigma_{bar} = \sigma[(t_1 + t_2)/2)] = \frac{1}{2}[2\sigma^2_{single}]^{1/2} = \frac{\sigma_{single}}{\sqrt{2}} \quad (3)$$

where σ_{single} is the time resolution of either SiPM on a bar. The time resolution of the difference of left and right SiPM within a bar is then given by:

$$\sigma_{t1-t2} = [2\sigma^2_{single}]^{1/2} = 2\sigma_{bar} \quad (4)$$

From the above equation bar resolution is given by the time resolution of the difference of left and right SiPM over 2.

3 Results and Analysis

3.1 Time Resolution without DCR noise

Figure 8 shows the distribution of the time difference for a particular delay and threshold setting that fitted to a Gaussian distribution to find the sigma of the distribution.

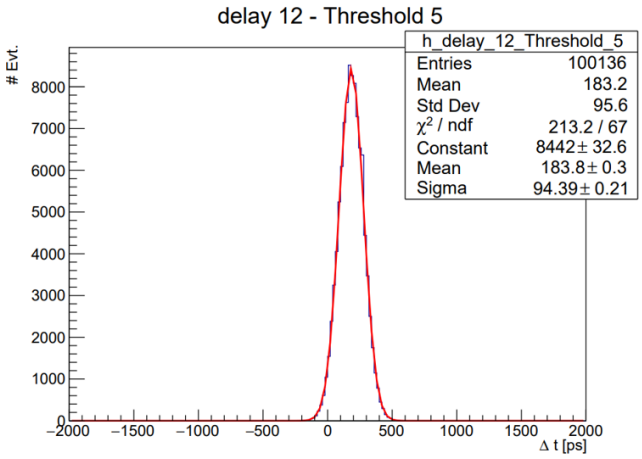

Figure 8. Distribution of the time difference with a Gaussian fit for 6000 photoelectrons at a particular delay and threshold values.

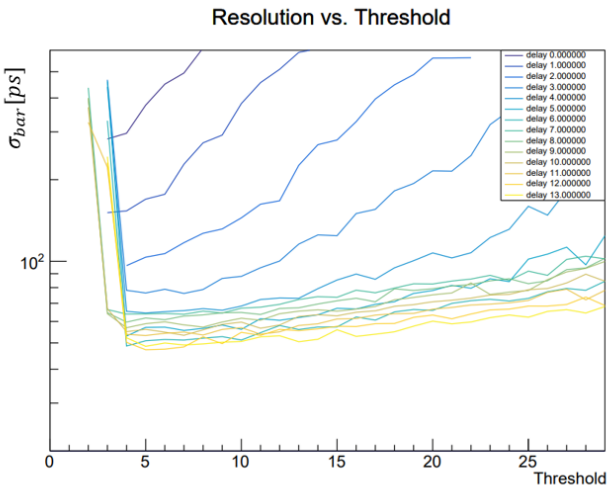

Figure 9. Bar resolution vs the threshold for different delays that are represented by the colors. This plot was made for 6000 photoelectrons.

Figure 9 shows the bar resolution, σ_{bar}, as a function of the threshold for all delays settings. At lower threshold (above the noise) the time resolution is better due to faster pulse slew rate, while at higher threshold the time resolution resolution is degraded due to slower slew rate and also LYSO photo-statistics.

We also analyzed the pulse shape for different delays and different number of photoelectrons. As expected we conclude that the pulse shape is bigger in amplitude when the

number of photoelectrons is higher. Also, the pulse amplitude and the width increase with the delay.
The dependency of the bar resolution to the number of photoelectron was also studied. A Different number of photoelectron was obtained by changing the laser tune and measure the voltage drop across the 240Ω resistor.
Results for different number of photoelectrons at a specific threshold and delay setting, using a frequency of 100kHz and 19ºC temperature are summarized in table 2.

Table 2. Summary of the time resolution and the slew rate measured for different number of photoelectrons.

Npe	$V_{drop}(mV)$	σ_{bar}(ps)	SR($\mu A/ns$)
4000	2.81	64.5 ± 0.2	6.61 ± 0.42
6000	4.22	47.2 ± 0.1	10.57 ± 0.40
8000	5.62	36.8 ± 0.1	14.30 ± 0.39

Note that the MIP particles produce around 6000 photoelectrons, so the values for that number of photoelectrons are the most important ones.
Next we want to see how the slew rate of the pulse shape varies with the number of photoneletrons and how that is related to the resolution. To find out the slew rate we need to find out the slope of the rising edge of the pulse. For that we made an histogram with the time distribution for each delay and threshold, then we fitted the plot with a gaussian and calculated the mean value. With this values we plotted the threshold as a function of the time mean value and made a fit of the plot, which is a straight line (figure 10). So, the slew rate (SR) is given by: $SR = slope \times 313$, where $313\mu A$ is the current value for range 0. In addition, we know that there is a relation between the time resolution and the slew rate, which is given by:

$$\sigma_{time} = \frac{\sigma_{noise}}{SR} \tag{5}$$

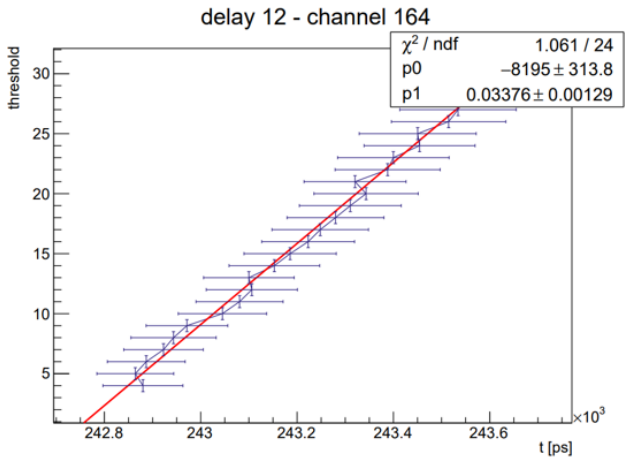

Figure 10. Plot shows the threshold vs the mean value of the crossing time distribution at each threshold. Using a linear fit the slew rate of the pulse is calculated.

In table 2 we can see that the slew rate is higher for a higher number of photoelectrons, this makes sense because the pulse shape is higher in amplitude, so the rising edge of the pulse should have a bigger slope. In equation 5 we can see that if the slew rate is higher then the resolution is smaller, which is in agreement with values on table 2.

3.2 Time Resolution with DCR noise

To study the time resolution with the DCR noise we emulated different DCR frequencies with the LED, all of them with the laser tuned for 6000 phothonelectrons. The results are summarized in table 3. As expected the time resolution gets worsen by increasing the DCR noise.

Table 3. Bar time resolution with different frequencies of the DCR noise

DCR frequency(GHz)	$V_{drop}(mV)$	σ_{bar}(ps)
5	35.1	48.19 ± 0.34
10	70.3	52.55 ± 0.35
15	105.4	57.85 ± 0.40
20	140.5	56.50 ± 0.40
25	175.7	61.40 ± 0.45
30	210.8	68.0 ± 0.5

4 Conclusion

After analyzing all the results we concluded that for 6000 photoelectrons the best resolution we got is $\sigma_{bar} = 47.2ps$, which is for a thereshold of 5 and a delay of 12. For 6000 photoelectrons and 30 GHz DCR noise we obtained $\sigma_{bar} = 68ps$. The results are lightly worse than the expected values from simulation. The source of the noise is already understood and is in the baseline holder of this new version of the chip. The problem will be fixed in the next version. Note that in the results of the resolution on table 3 you can see that the absolute uncertainty of the resolution values is getting higher with the DCR frequency which means that there is more dispersion of the values with the increase of the DCR frequency. In addiction, in table 3 you can see that the relative uncertainty is around 7% for all the frequencies, which makes sense because this values were acquire in the same conditions. However, on table 2 for 6000 photoelectrons we have that the relative uncertainty for the time resolution is around 2% which is less than the values on table 3. This can happen, because this value was not taken on the same day as the other ones and so there could be some small variations in the alignment of the laser and in the ASIC channel response, that could influence the results.

References

[1].CMS Collaboration, Technical Design Report of the MIP Timing Detector for the CMS Phase-2 Upgrade, 15 Mar 2019, CERN-LHCC- 2019-003; CMS-TDR-020.
[2].T. Niknejad, Precision timing with the cms mtd barrel timing layer for hl-lhc, LIP Seminar (2021).
[3].T. Niknejad, TOFHIR2A test results, March.31, 2021